Article

Chinese Science Bulletin

Geology

February 2012 Vol.57 No.6: 651–659
doi: 10.1007/s11434-011-4852-x

Repeated modification of lithospheric mantle in the eastern North China Craton: Constraints from SHRIMP zircon U-Pb dating of dunite xenoliths in western Shandong

YANG DeBin[1,2*], XU WenLiang[1*], GAO Shan[3], XU YiGang[2] & PEI FuPing[1]

[1] *College of Earth Sciences, Jilin University, Changchun 130061, China;*
[2] *CAS Key Laboratory of Isotopic Geochronology and Geochemistry, Guangzhou Institute of Geochemistry, Chinese Academy of Sciences, Guangzhou 510640, China;*
[3] *State Key Laboratory of Geological Processes and Mineral Resources, China University of Geosciences, Wuhan 430074, China*

Received June 7, 2011; accepted October 10, 2011; published online November 21, 2011

Four dunite xenoliths from the Tietonggou intrusion of western Shandong, China, were subjected to SHRIMP zircon U-Pb dating to constrain timing of the North China Craton (NCC) destruction, a topic of much controversy. Cathodoluminescence images revealed that 15 of the 18 zircon grains from the xenoliths display striped absorption. The rest showed oscillatory growth zoniation. All the zircons had variable contents of Th (49–3569 ppm; average, 885 ppm) and U (184–5398 ppm; average, 1277 ppm), and variable Th/U ratios (0.15–2.04). These zircon characteristics indicate a magmatic origin. The zircon age data can be divided into five groups: 131–145, 151–164, 261–280, 434–452, and 500–516 Ma. Group I (131–145 Ma) is consistent with timing of formation of the Tietonggou high-Mg diorites. Group II (151–164 Ma) is similar in age to Middle-Late Jurassic magmatism in the eastern NCC, which included both mantle-derived and intensive crust-derived magmatism. Group III (261–280 Ma) is similar in age to the Emeishan large igneous province, and Group IV (434–452 Ma) is similar in age to Paleozoic high-silica magmatism in the eastern NCC. Group V (500–516 Ma) may correspond to the global Pan-African event. Results indicate repeated modification of lithospheric mantle in the eastern NCC, and suggest that the most intensive modification occurred in the late Mesozoic (131–164 Ma).

dunite, SHRIMP zircon dating, lithospheric mantle, multiple modification, North China Craton

Citation: Yang D B, Xu W L, Gao S, et al. Repeated modification of lithospheric mantle in the eastern North China Craton: Constraints from SHRIMP zircon U-Pb dating of dunite xenoliths in western Shandong. Chin Sci Bull, 2012, 57: 651–659, doi: 10.1007/s11434-011-4852-x

The Archean North China Craton (NCC) is an ideal setting in which to investigate the destruction of a stable craton. The lithospheric mantle beneath the NCC underwent a dramatic change from an ancient, cold, and >200-km-thick lithospheric mantle in the Early Paleozoic to a young, hot, and 60–80-km-thick lithospheric mantle in the Cenozoic [1–11]. This change in thickness has been referred to as lithospheric thinning or craton destruction. However, there are uncertainties and controversy regarding the timing of this lithospheric thinning, the geodynamic context of this event, and the mechanism of the thinning. Previous studies have proposed that NCC destruction occurred during the Mesozoic [7,12–14], the Late Mesozoic [15–18], or the Mesozoic and Cenozoic [19], based mainly on analyses of Mesozoic and Cenozoic magmatism in the eastern NCC and in the Dabie-Sulu orogenic belt. However, few geochronological data have been reported for the modified lithospheric mantle in this region.

Early Cretaceous high-Mg diorites in western Shandong contain harzburgite xenoliths with Archean Re-depletion model ages and abundant dunite xenoliths [20–24]. Trace element data of minerals and whole-rock Sr-Nd-Os isotopic data of the Tietonggou peridotite xenoliths (from Early Cretaceous high-Mg diorites) reveal that the harzburgites

*Corresponding authors (email: yangdb@jlu.edu.cn; xuwl@jlu.edu.cn)

represent the residue of ancient lithospheric mantle; whereas, the dunites formed *via* a reaction between mantle peridotite and melt derived from delaminated lower continental crust [24,25]. In this case, zircons in the xenoliths are likely to have formed during modification of the lithospheric mantle by a silicate-rich melt.

The present study aims to constrain timing of the NCC destruction, based on detailed petrographic studies of four dunite xenoliths entrained by Early Cretaceous high-Mg diorites in western Shandong, as well as SHRIMP zircon U-Pb age data. The data constrain the timing of modification of lithospheric mantle beneath the eastern NCC.

1 Geological background and sample descriptions

The NCC – surrounded by the Central Asian Orogenic Belt (CAOB), the Qinling-Dabie-Sulu orogenic belt, and the Yangtze Craton (YC) (Figure 1(a)) – is subdivided into the Eastern Block, Western Block, and intervening Trans-North China Orogen (TNCO)/Central Orogenic Belt based on the age and lithological associations of metamorphic rocks, tectonic evolution, and the *P-T-t* path of metamorphism [26].

Western Shandong, located in the Eastern Block of the NCC (Figure 1(a)), is dominated by the Archean Taishan Group, Cambrian and Lower-Middle Ordovician series, and Carboniferous-Permian sequences. Mesozoic strata are dominant and consist mainly of sedimentary rocks in grabens, while Cenozoic strata consist mainly of alluvial and lacustrine sediments [27]. In addition to Precambrian igneous rocks, voluminous Mesozoic intrusive rocks are widespread throughout western Shandong. The Tietonggou intrusion, which is exposed over an area of approximately 5 km^2 (Figure 1(b)), is located near Yanzhuang town in Laiwu city (117°52′E, 36°05′N), and consists mainly of early norite-gabbro and later pyroxene-diorite. Results of laser ablation-inductively coupled plasma-mass spectrometry (LA-ICP-MS) zircon U-Pb dating and biotite Ar-Ar dating indicate that the Tietonggou pyroxene-diorite formed in the Early Cretaceous (131–135 Ma) [28,29].

Peridotite xenoliths are abundant in the Tietonggou intrusion, and are generally ellipsoidal, ranging in size from 3 cm × 2 cm × 1 cm to 8 cm × 6 cm × 4 cm (Figure 2(a)). Based on their contents of olivine, orthopyroxene, and clinopyroxene, the xenoliths can be classified into chromite-bearing dunite, spinel-bearing harzburgite, and chromite-bearing wehrlite. The dunite is dominant [24]. This study is focused exclusively on chromite-bearing dunites from the Tietonggou intrusion.

The chromite-bearing dunites are green in color and are equigranular and/or porphyroclastic, or massive, and consist of olivine (~93%), chromite (~3%), orthopyroxene (~3%), and phlogopite (~1%) (Figure 2(b)–(d)). Olivines can be subdivided into two groups, based on their size. Group I consists of porphyroclastic olivines with kink bands, ranging in size from 1.0 to 4.0 mm; Group II consists of unstrained recrystallized olivines ranging in size from 0.3 to 0.6 mm. The dunites are cut by veins of orthopyroxene ± phlogopite. Secondary clinopyroxenes occur locally around chromite within the dunites. The mineralogy and petrography of the dunites have been described previously [24].

2 Methods

To avoid contamination of dunite xenoliths by the host rocks, a detailed petrographic study was performed initially. The weathered surfaces of the xenoliths and reaction rims between

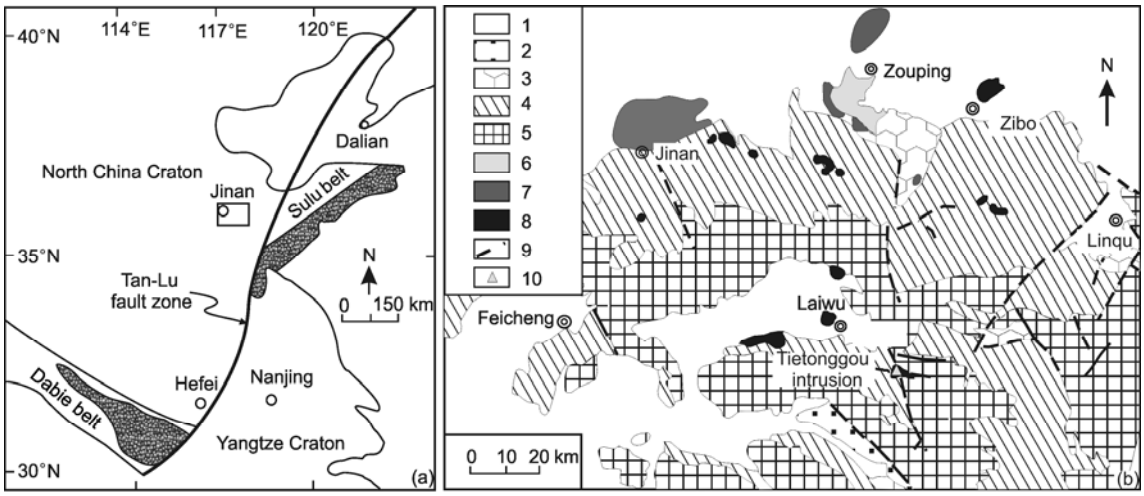

Figure 1 Geological sketch map of the western Shandong (modified after [29]). 1, Quaternary system; 2, Paleogene-Neogene system; 3, Mesozoic Erathem; 4, Paleozoic Erathem; 5, Archean Eonothem; 6, Mesozoic volcanic rocks; 7, gabbro; 8, diorite; 9, fault; 10, sampling location.

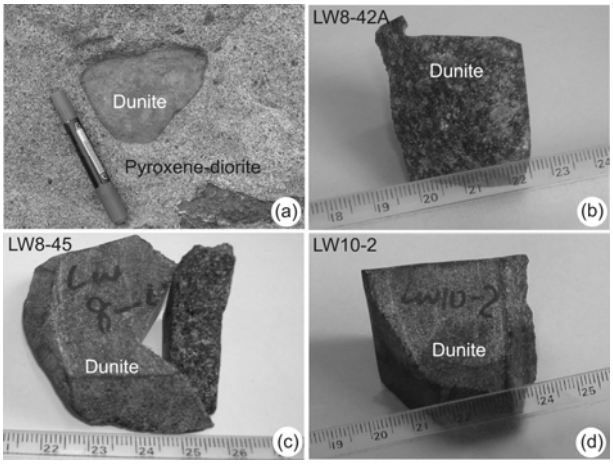

Figure 2 Photographs showing field occurrence and textures of dunite xenoliths from the western Shandong.

the xenoliths and host rocks were removed using a diamond saw. The remaining rock was manually crushed to 100–120 mesh and washed with ethanol. After magnetic separation, zircons were concentrated using heavy liquid, and finally hand-picked under a binocular microscope. Except for the magnetic separation device, new tools were used to avoid contamination of the samples during the separation of zircon. Zircon grains were mounted in epoxy, polished, and coated with gold. The grains were examined under transmitted and reflected light using an optical microscope, and cathodoluminescence (CL) images were obtained using a JEOL scanning electron microscope housed at the Beijing Ion-probe Center, Chinese Academy of Geological Sciences, Beijing, China, to reveal their internal structures and to select suitable sites for SHRIMP analyses. The zircons were analyzed using a SHRIMP II at the Beijing Ion-probe Center, Chinese Academy of Geological Sciences, Beijing, China. Details of the experimental conditions and procedures have been described previously [30–32]. Ages were calibrated against a reference zircon (TEM) with an age of 417 Ma [33]. U, Th, and Pb concentrations were measured using the reference zircon SL13 (age of 572 Ma; U content of 238 ppm). Data were calculated using SQUID 1.0 and ISOPLOT 3.0 programs [34]. Common Pb was corrected based on the measured ^{208}Pb. Ablation pits were generally about 25 μm × 30 μm in area.

3 Results

We obtained 7 zircon grains from ~300 g of sample LW8-42A, 5 grains from ~280 g of sample LW8-42B, 5 from ~250 g of sample LW8-45, and 2 from ~270 g of sample LW10-2. Analytical results for the samples are given in Table 1.

Zircons from sample LW8-42A were transparent and

Table 1 SHRIMP zircon U-Pb dating results for the dunite xenolithes [a)]

Spot No.	$^{206}Pb_c$ (%)	U (ppm)	Th (ppm)	Th /U	^{206}Pb* (ppm)	^{206}Pb/^{238}U age (Ma)	^{207}Pb*/^{206}Pb*	±%	^{207}Pb*/^{235}U	±%	^{206}Pb*/^{238}U	±%	Err. corr.
Sample LW8-42A													
1	0.20	315	292	0.96	11.2	261.0±11	0.0570	3.3	0.324	4.8	0.0413	3.5	0.721
2	2.68	335	49	0.15	7.46	151.3±6.1	0.0533	9.5	0.175	10	0.0238	3.5	0.347
3	0.29	388	191	0.51	24.5	452.0±17	0.0553	2.8	0.554	4.5	0.0727	3.4	0.771
4	0.90	1368	1366	1.03	24.2	130.6±5.4	0.0539	2.2	0.152	4.1	0.0205	3.5	0.843
5	2.23	1161	1549	1.38	23.9	145.3±7.0	0.0484	4.4	0.152	5.6	0.0228	3.5	0.621
6	0.58	3587	1299	0.37	68.6	141.4±5.0	0.0501	2.9	0.153	4.4	0.0222	3.4	0.762
7	2.50	699	330	0.49	14.0	143.6±5.7	0.0513	7.2	0.160	8.0	0.0225	3.5	0.437
Sample LW8-42B													
1	3.52	951	234	0.25	22.7	158.2±6.8	0.0518	15	0.178	15	0.0249	3.5	0.236
2	0.49	5398	1301	0.25	103	140.6±4.8	0.0512	1.7	0.156	3.7	0.0221	3.3	0.891
3	1.63	2102	1398	0.69	48.3	164.3±6.5	0.0524	5.1	0.187	6.1	0.0258	3.4	0.558
4	0.46	1460	812	0.57	27.5	139.1±5.1	0.0531	2.3	0.160	4.1	0.0218	3.4	0.825
Sample LW8-45													
1	0.86	1980	2925	1.53	41.0	152.1±6.9	0.0691	4.2	0.227	5.4	0.0239	3.4	0.630
2	0.74	1804	3569	2.04	33.2	139.0±7.6	0.0760	3.2	0.228	4.9	0.0218	3.7	0.752
3	0.86	824	359	0.45	60.2	514.0±18.0	0.0588	2.7	0.673	4.3	0.0830	3.4	0.782
4	3.14	237	212	0.92	11.6	322.0±18.0	0.0700	21	0.490	22	0.0512	4.2	0.192
5	1.60	234	88	0.39	9.59	280.0±12.0	0.0544	6.5	0.333	7.5	0.0445	3.6	0.486
Sample LW10-2													
1	0.78	228	240	1.09	16.2	500.3±9.9	0.0657	10	0.731	10	0.0807	1.5	0.149
2	0.35	1011	427	0.44	72.5	515.8±3.8	0.0612	1.2	0.703	1.4	0.0833	0.72	0.500
3	1.99	184	166	0.93	11.2	433.6±6.9	0.0620	5.6	0.595	5.8	0.0696	1.3	0.229

a) Errors in 1σ; Pb_c and Pb* indicate the common and radiogenic portions, respectively. Error in Standard calibration was 1.78%; common Pb corrected using measured ^{208}Pb.

possessed elliptical or irregular shapes. The grains were 35–110 μm in length and had length/width ratios of 1.1–2.0 (Figure 3(a)). The $^{206}Pb/^{238}U$ ages obtained for 4 of 7 analytical spots from sample LW8-42A ranged from 131 to 145 Ma. These zircons displayed striped absorption in CL images (Figure 3(a)), similar to those reported for mafic igneous rocks and the host diorite [29]. The Th and U contents of the zircons varied from 330 to 1549 ppm and from 699 to 3587 ppm, respectively, and their Th/U ratios ranged from 0.37 to 1.38 (Figure 4). The spot 2 zircon, which yielded an age of 151 Ma, showed typical magmatic oscillatory growth zonation. The spot 1 and 3 zircons, which had striped absorption and Th/U ratios of 0.95 and 0.51, yielded $^{206}Pb/^{238}U$ ages of 261±11 and 452±17 Ma, respectively (Figure 5(a)).

Zircons from sample LW8-42B, which were colorless/transparent and prismatic to elliptical in shape, were 40–100 μm long and had length/width ratios of 1.5–2.5 (Figure 3(b)). Two of the 4 analyzed spots in this sample yield $^{206}Pb/^{238}U$ ages of 139±5 (spot 4) and 141±5 Ma (spot 2) (Figure 5(b)), consistent with the youngest ages of zircons from sample LW8-42A. These two zircons showed striped absorption in CL images (Figure 3(b)) and had high U contents (1460 and 5398 ppm) and high Th/U ratios (0.57 and 0.25) (Figure 4), indicating a magmatic origin. The other two zircons yielded $^{206}Pb/^{238}U$ ages of 158±7 and 164±7 Ma, showed weakly striped absorption in CL images, had high contents of Th (234 and 1398 ppm) and U (951 and 2102 ppm), and high Th/U ratios (0.25 and 0.69) (Figure 4).

Zircons from sample LW8-45 were colorless/transparent and stubby to acicular or irregular in shape. The grains were

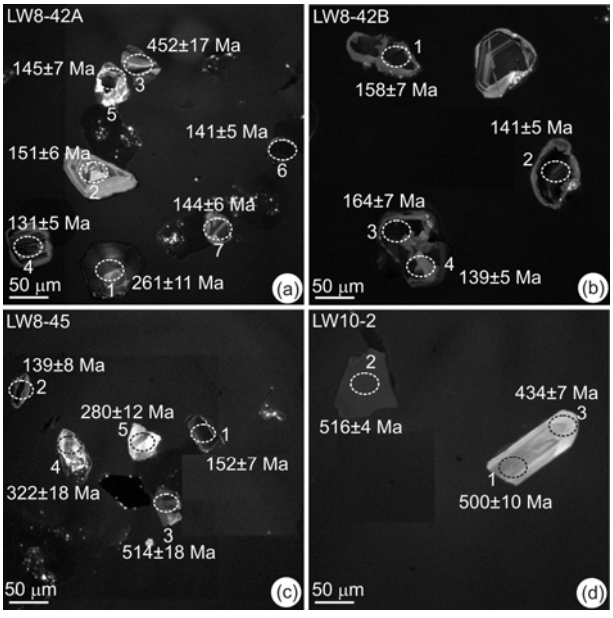

Figure 3 Cathodoluminescence (CL) images of zircons for dunite xenoliths. Ellipses indicate analysis sites. Numbers indicate analytical spot number and $^{206}Pb/^{238}U$ age.

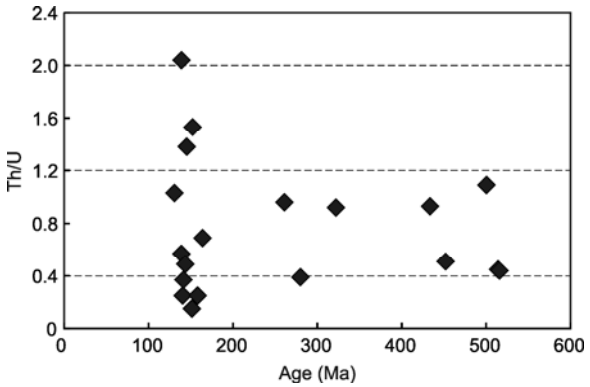

Figure 4 Plots of zircon Th/U ratios *vs*. their U-Pb ages for dunite xenoliths.

40–70 μm long and had length/width ratios of 1.3–2.0 (Figure 3(c)). All 5 of the analyzed spots plotted on or near a concordia curve (Figure 5(c)). Two of the grains yielded $^{206}Pb/^{238}U$ ages of 139±8 and 152±7 Ma, showed striped absorption in CL images (Figure 3(c)), had high contents of Th (3569 and 2925 ppm) and U (1804 and 1980 ppm), and high Th/U ratios (2.04 and 1.53) (Figure 4), indicating a magmatic origin. The other three spots (Spots 3–5) yielded $^{206}Pb/^{238}U$ ages of 514±18, 322±18, and 280±12 Ma, respectively (Figure 5(c)). These zircons were characterized by relatively low contents of Th (88–359 ppm) and U (234–824 ppm), and low Th/U ratios (0.39–0.92) (Figure 4).

Zircons selected from sample LW10-2 were 70–150 μm in length, colorless/transparent, and prismatic or irregular in shape (Figure 3(d)). Three spots were analyzed on two zircon grains from the sample. The core and rim of one grain yielded $^{206}Pb/^{238}U$ ages of 500±10 and 434±7 Ma, respectively (Figure 5(d)). The zircon showed striped absorption in CL images (Figure 3(d)) and yielded Th/U ratios for the core and rim of 1.09 and 0.93, respectively (Figure 4). The other zircon grain (spot 2) from the sample is structureless in a CL image, had a high U content (1011 ppm) and a high Th/U ratio (0.44), and yielded a $^{206}Pb/^{238}U$ age of 516±4 Ma.

4 Discussion

4.1 Origin of zircon in dunite xenoliths

Zircon ($ZrSiO_4$) grows under SiO_2-oversaturated conditions. Primary zircon does not readily form in mantle peridotite because of the extremely low Zr and Si contents of this rock type. However, zircon has been reported from ultrahigh-pressure garnet peridotites and mantle-derived peridotite xenoliths [35–41]. The growth of zircons in such xenoliths may be related to late-stage modification of mantle peridotite by silica-rich melts [35,36]. Thus it is relevant whether dunite xenoliths from the Tietonggou high-Mg diorites were modified by silica-rich melt. In the case of the Tietonggou peridotite xenoliths, evidence of such modification may be obtained from petrographic studies, *in situ* mineral trace

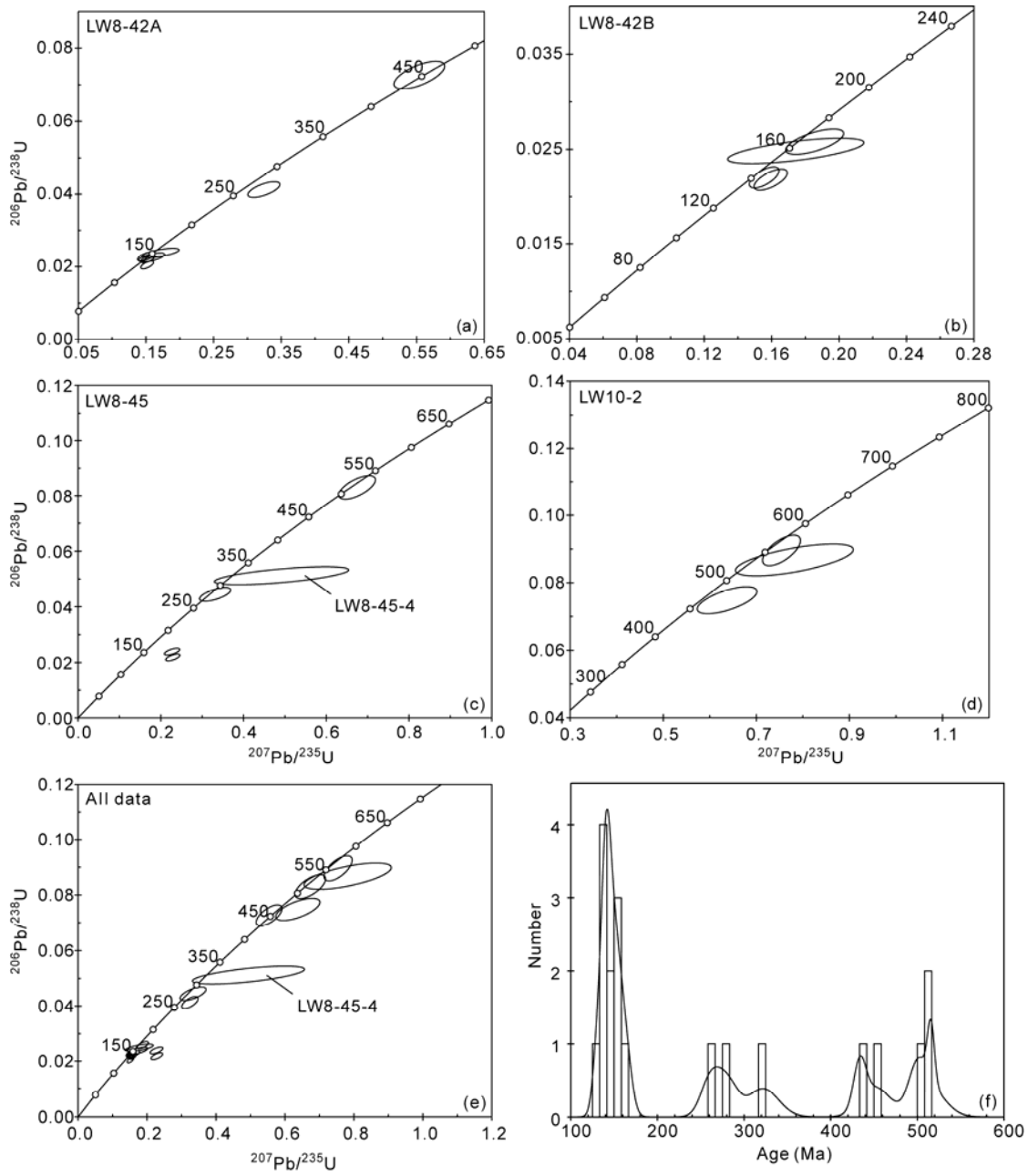

Figure 5 U-Pb Concordia diagrams (a)–(e), and relative probability diagram (f) of the SHRIMP zircon U-Pb for dunite xenoliths.

element data, and whole-rock Sr-Nd-Os isotopic data. In these dunite xenoliths, metasomatized orthopyroxene and orthopyroxene + phlogopite occur as veins or zoning around chromite, suggesting that the xenoliths were indeed modified by silica-rich melt [22,24]. In addition, the orthopyroxene that occurred in veins and around chromite had higher contents of trace earth elements than primary orthopyroxene from the harzburgite xenoliths. Secondary clinopyroxene in wehrlite xenoliths was strongly enriched in light rare earth elements and depleted in heavy rare earth elements [24]. Finally, the dunite xenoliths were characterized by high initial $^{87}Sr/^{86}Sr$ ratios (0.7058–0.7212), low $\varepsilon_{Nd}(t)$ values (−19.59 to +0.18), and clear Re addition. These lines of evidence suggest that the dunite xenoliths were modified by silica-rich melt [24,25].

Combined with the existence of harzburgite xenoliths with Archean Re-depletion model ages in the same intrusion, and trace element abundances of olivines from the dunite xenoliths [22,24], we conclude that the dunite xenoliths originated in the lithospheric mantle, but were strongly modified by melt derived from the delaminated continental crust [24]. Zircons in the dunite xenoliths could be attributed to modification by such a silica-rich melt. In other words, the different groups of zircon ages may represent events in

which silica-rich melts modified the lithospheric mantle.

4.2 Origin of zircons in dunite xenoliths

The SHRIMP zircon U-Pb age data from the four dunite xenoliths, except for spot 4 in sample LW8-45-4 (322± 18 Ma), which yielded a large error, can be subdivided into five groups: 131–145 Ma ($n=7$), 151–164 Ma ($n=4$), 261–280 Ma ($n=2$), 434–452 Ma ($n=2$), and 500–516 Ma ($n=3$) (Figure 5(e), (f)). Group 1 (131–164 Ma) was dominant in dunite xenoliths and was similar in age to the intrusive age of the host rocks (Tietonggou intrusion; 131–134 Ma) [28,29], which may indicate strong interaction between melt derived from the delaminated lower continental crust and mantle peridotite.

Previous studies have reported that delamination of the lower continental crust beneath the NCC was possibly related to collision between the NCC and Yangtze blocks during the Triassic (220–240 Ma) [14,24,42], and that interaction between silica-rich melt and mantle peridotite occurred after this time. In this case, the question would remain regarding the origin of zircons in the dunites xenoliths that yielded ages of 261–280, 434–452, and 500–516 Ma. There are two possible zircon origins of these ages: (1) they originated from the delaminated lower continental crust of the NCC and/or the subducted slab of the YC; or (2) they were derived from repeated modification of the lithospheric mantle by silica-rich melts. In the first case, we would have expected to find zircons with ages of 2500 Ma, 1850 Ma (typical of the NCC) and/or 700–900 Ma (typical of the YC). However, zircons with these ages were not found in the dunite xenoliths. Thus, we conclude that these zircons record repeated modification of lithospheric mantle. This interpretation gives rise to the question of whether coeval magmatism, similar to the ages of zircons in the dunite xenoliths, existed in the eastern NCC.

Magmatic zircons are generally distinguished from metamorphic zircons based on cathodoluminescence (CL) images and Th and U contents of zircon, as well as their Th/U ratios [43]. Typically, magmatic zircons show oscillatory growth zonation (for felsic igneous rocks) or striped absorption (for mafic igneous rocks) in CL images, and have high Th and U contents, and high Th/U ratios (>0.4). Conversely, metamorphic zircons are structureless or show pudding texture on CL images and have low Th and U contents, as well as low Th/U ratios (<0.1) [43–47].

In the present study, zircons with ages of 131–145 Ma in dunite xenoliths were subhedral or anhedral, showing clear striped absorption in CL images. They also had high Th/U ratios (0.25–2.04), indicating a magmatic origin. The weighted mean $^{206}Pb/^{238}U$ age of 139±4 Ma (MSWD = 0.75) for seven spots is consistent with timing of formation of the Tietonggou high-Mg diorites (131–135 Ma) [28,29] within error, suggesting that the zircons formed during a period of intensive interaction between delaminated lower continental crust-derived melt and mantle peridotite. These ages also are consistent with the timing of large-scale mantle- and crust-derived magmatism in the eastern NCC during the Early Cretaceous, such as the Jinling, Yi'nan (Shangyu), and Ji'nan intrusions in western Shandong (127–134 Ma) [29, 48–50]; the Liguo, Jiagou, Banjing, Fengshan, and Caishan intrusions in Xuzhou-Huaibei (127–132 Ma) [51,52]; and granitoids in eastern Shandong and eastern Liaodong (120–130 Ma) [53–55].

The group of zircons from dunite xenoliths with ages of 151–164 Ma yielded a weighted mean $^{206}Pb/^{238}U$ age of 156±7 Ma (MSWD = 0.78, $n = 4$). These zircons showed striped absorption and oscillatory growth zonation in CL images, and had Th/U ratios of 0.15 to 1.53, suggesting a magmatic origin. Although spot 2 in sample LW8-42A had a low Th/U ratio (0.15), it showed typical oscillatory growth zonation, again indicating a magmatic origin. Based on these findings, we conclude that the zircons with ages of 151–164 Ma are of magmatic origin. These ages (151–164 Ma) are consistent with the SHRIMP zircon U-Pb age of the Huaziyu mafic lamprophyre in eastern Liaoning province (155±4 Ma) [56], and with zircon U-Pb ages of the Jingshan granitoids in the Bengbu area, the Duogushan and Wendeng granitoids in the northern section of the Sulu ultrahigh-pressure metamorphic belt (155–160 Ma) [54,57], the Linglong and Luanjiahe granitoids in eastern Shandong (155–160 Ma) [53], and Late Jurassic granitoids in eastern Liaoning [58]. Late Jurassic magmatism in the eastern NCC was generally characterized by intensive felsic magmatic events, whereas little mafic magmatism occurred at this time (e.g. the Huaziyu lamprophyre in the eastern Liaoning).

The zircons with ages of 261–280 Ma were subhedral or anhedral, showed striped absorption in CL images, and had high Th/U ratios (0.39–0.96), suggesting a magmatic origin. The age group of 261–280 Ma was similar to the age of the Emeishan large igneous province (259–262 Ma) [59,60] and corresponds with timing of the mass extinction event at the end of the Permian [61]. Permian igneous rocks have not been reported from the eastern NCC, except for a small quantity of detrital zircons (ages of 273–282 Ma) extracted from Jurassic sandstones in the Mengyin and Zhoucun basins [62]. SHRIMP and LA-ICP-MS zircon U-Pb age data for felsic intrusive rocks, volcanic tuff, and mafic-ultramafic rocks indicate magmatism at 254–285 Ma along the northern margin of the NCC [63–66]. These results suggest that the global Permian event affected not only the northern margin of the NCC, but also the lithospheric mantle beneath the eastern NCC.

Zircons of the present study with ages of 434–452 Ma showed striped absorption in CL images and had high Th/U ratios (0.51–0.93), suggesting a magmatic origin. These ages are consistent with the LA-ICP-MS U-Pb ages of captured zircons from the Xiachangzhuang magnetite–amphibolite intrusive rock (450–484 Ma) [67], SIMS U-Pb ages of captured magmatic zircons with oscillatory growth zonation

from Cenozoic basalt in eastern Liaoning (419–487 Ma) [68], and the U-Pb age of perovskites from the Mengyin kimberlite in western Shandong Province (456±8 Ma) [69], as well as phlogopite Rb-Sr and Ar-Ar ages obtained for the Fuxian kimberlite in the Liaoning region (463–466 Ma) [70,71]. These results point to the occurrence of Paleozoic magmatic events in the eastern NCC. The ultramafic nature of kimberlites hampers the formation of zircon. However, the presence of zircons that grew within kimberlitic magma in western Shandong and eastern Liaodong indicates the occurrence of a silica-rich magmatic event in the eastern NCC, in addition to early Paleozoic silica-poor ultramafic magmatism. Early Paleozoic zircons from dunite xenoliths, as analyzed in the present study, may have resulted from metasomatism of a silica-rich melt.

As mentioned above, zircons with ages of 500–516 Ma were of magmatic origin. These ages were similar to those of the Pan-African tectono-thermal events, indicating that the lithospheric mantle underneath the eastern NCC was affected by this event. Until now, this period of magmatism had only been reported in captured zircons from the Xiachangzhuang magnetite–amphibolite intrusion (505±10 Ma) [67] and in detrital zircons from Cretaceous sedimentary rocks (497±13 Ma) in the Pingyi Basin of western Shandong [62].

4.3 Repeated modification of the lithospheric mantle in the eastern NCC

Results of SHRIMP zircon U-Pb dating of the Tietonggou dunite xenoliths indicate that lithospheric mantle in western Shandong records multiple episodes of mantle magmatism ranging in age from the early Paleozoic to the late Mesozoic (131–516 Ma). This observation indicates that the lithospheric mantle was subjected to various degrees of melt-related modification, and that the most intensive modification occurred in the late Mesozoic (131–164 Ma).

Recent studies of peridotite xenoliths from Paleozoic diamond-bearing kimberlites and Cenozoic basalts have revealed that the lithospheric mantle in the NCC has experienced a complex evolutionary process [72–75]. For example, Li, Sr, and Nd isotopic data for peridotite xenoliths from the Hannuoba, Fanshi, and Hebi Cenozoic basalts within the NCC suggest that lithospheric mantle in the NCC experienced multiple interactions between melt/fluid and peridotite [72]. The repeated modification of lithospheric mantle in the NCC is indicated by zircon U-Pb dating, trace element data, and Hf isotopic data for garnet/spinel pyroxenite veins that formed *via* reactions between a silica-rich melt and peridotite in the Cenozoic Hannuoba basalts [73], and by *in situ* Re-Os isotopic data on sulfides from peridotite xenoliths in these basalts [74]. Petrographic and mineral chemical data for pyroxenes from garnet peridotite xenoliths in the Mengyin kimberlites revealed that the ancient lithospheric mantle in the eastern NCC has been repeatedly overprinted [75].

Results reported herein suggest that the lithospheric mantle in the eastern NCC has been repeatedly modified and that the most intensive modification occurred in the late Mesozoic (131–164 Ma).

5 Conclusions

(1) Zircons from dunite xenoliths in the Tietonggou intrusion of western Shandong formed during repeated modification of the lithospheric mantle by silica-rich melt.

(2) SHRIMP zircon U-Pb age data indicate that all the zircons are of magmatic origin, and yield ages that define five groupings: 131–145, 151–164, 261–280, 434–452, and 500–516 Ma, consistent with the occurrence of multiple magmatic-thermal events in the eastern NCC.

(3) The lithospheric mantle in the eastern NCC was subjected to repeated modification, with the most intensive modification occurring in the late Mesozoic (131–164 Ma).

We appreciate the assistance of Director Li Linqing of the Langfang Geological Survey of Hebei Province for technical support during sample collection. We thank Song Biao and Liu Dunyi for technical support during SHRIMP II analyses. We appreciate comments by two anonymous reviewers which improved the manuscript. This work was supported by the National Basic Research Program of China (2009CB825005), the National Natural Science Foundation of China (90814003, 90714010, 91014004 and 41002018).

1 Fan W M, Menzies M A. Destruction of aged lower lithosphere and accretion of asthenosphere mantle beneath eastern China. Geotect Metal, 1992, 16: 171–180
2 Menzies M A, Fan W M, Zhang M. Palaeozoic and Cenozoic lithoprobes and the loss of >120 km of Archaean lithosphere, Sino-Korean craton, China. In: Prichard H M, Alabaster T, Harris N B W, eds. Magmatic Processes and Plate Tectonics. London: Geol Soc London Spec Public, 1993. 76: 71–81
3 Menzies M A, Xu Y G, Zhang H F, et al. Integration of geology, geophysics and geochemistry: A key to understanding the North China Craton. Lithos, 2007, 96: 1–21
4 Griffin W L, Zhang A D, O'Reilly S Y, et al. Phanerozoic evolution of the lithosphere beneath the Sino-Korean Craton. In: Flower M F J, Chung S L, Lo C H, et al. eds. Mantle Dynamics and Plate Interactions in East Asia. Amer Geophys Union Geodyn Ser, 1998, 27: 107–126
5 Zheng J P, O'Reilly S Y, Griffin W L, et al. Nature and evolution of Cenozoic lithospheric mantle beneath Shandong Peninsula, Sino-Korean Craton, Eastern China. Inter Geol Rev, 1998, 40: 471–499
6 Fan W M, Zhang H F, Baker J, et al. On and off the North China Craton: Where is the Archaean keel? J Petrol, 2000, 41: 933–950
7 Xu Y G. Thermo-tectonic destruction of the Archean lithospheric keel beneath the Sino-Korean Craton in China: Evidence, timing and mechanism. Phys Chem Earth, 2001, 26: 747–757
8 Gao S, Rudnick R L, Carlson R W, et al. Re-Os evidence for replacement of ancient mantle lithosphere beneath the North China craton. Earth Planet Sci Lett, 2002, 198: 307–322
9 Deng J F, Su S G, Niu Y L, et al. A possible model for the lithospheric thinning of North China Craton: Evidence from the Yanshanian (Jura-Cretaceous) magmatism and tectonism. Lithos, 2007, 96: 22–35
10 Zhang H F, Goldstein S L, Zhou X H, et al. Evolution of subconti-

nental lithospheric mantle beneath eastern China: Re-Os isotopic evidence from mantle xenoliths in Paleozoic kimberlites and Mesozoic basalts. Contrib Mineral Petrol, 2008, 155: 271–293
11 Wu F Y, Xu Y G, Gao S, et al. Lithospheric thinning and destruction of the North China Craton (in Chinese). Acta Petrol Sin, 2008, 24: 1145–1174
12 Menzies M A, Xu Y G. Geodynamics of the North China Craton. In: Flower M F J, Chung S L, Lo C H, et al., eds. Mantle dynamics and plate interaction in east Asia. Amer Geophys Union Geodyn Ser 27, 1998, 100: 155–164
13 Gao S, Luo T C, Zhang B R, et al. Chemical composition of the continental crust as revealed by studies in East China. Geochim Cosmochim Acta, 1998, 62: 1959–1975
14 Xu W L, Gao S, Wang Q H, et al. Mesozoic crustal thickening of the eastern North China Craton: Evidence from eclogite xenoliths and petrologic implications. Geology, 2006, 34: 721–724
15 Wu F Y, Sun D Y. The mesozoic magmatism and lithospheric thinning in eastern China (in Chinese). J Changchun Univ Sci Tech, 1999, 29: 313–318
16 Wu F Y, Ge W C, Sun D Y. Discussions on the lithospheric thinning in eastern China (in Chinese). Earth Sci Front, 2003, 10: 51–60
17 Chen B, Zhai M G. Geochemistry of late Mesozoic lamprophyre dykes from the Taihang Mountains north China and implications for the sub-continental lithospheric mantle. Geol Magazine, 2003, 140: 87–93
18 Chen B, Jahn B M, Arakawa Y, et al. Petrogenesis of the Mesozoic intrusive complexes from the southern Taihang orogen, North China Craton: Elemental and Sr-Nd-Pb isotopic constraints. Contrib Mineral Petrol, 2004, 148: 489–501
19 Xu W L,Wang D Y, Wang S M. PTtC model of mesozoic and cenozoic volcanisms and lithospheric evolution in eastern China (in Chinese). J Changchun Univ Sci Tech, 2000, 30: 329–335
20 Xu W L, Wang D Y, Gao S, et al. Discovery of dunite and pyroxenite xenoliths in Mesozoic diorite at Jinling, western Shandong and its significance. Chin Sci Bull, 2003, 48: 1599–1603
21 Xu W L, Wang D Y, Wang Q H, et al. Petrology and geochemistry of two types of mantle-derived xenoliths in Mesozoic diorite from western Shandong Province (in Chinese). Acta Petrol Sin, 2003, 19: 623–636
22 Xu W L, Wang D Y, Wang Q H, et al. Metasomatism of silica-rich melts (liquids) in dunite xenoliths from western Shandong, China: Implication for Mesozoic lithospheric mantle thinning (in Chinese). Acta Geol Sin, 2004, 78: 72–80
23 Chen L H, Zhou X H. Subduction-related metasomatism in the thinning lithosphere: Evidence from a composite dunite-orthopyroxenite xenolith entrained in Mesozoic Laiwu high-Mg diorite, North China Craton. Geochem Geophys Geosys, 2005, 6: Q06008
24 Xu W L, Hergt J M, Gao S, et al. Interaction of adakitic melt-peridotite: Implications for the high-Mg# signature of Mesozoic adakitic rocks in the eastern North China Craton. Earth Planet Sci Lett, 2008, 265: 123–137
25 Xu W L, Yang D B, Gao S, et al. Geochemistry of peridotite xenoliths in Early Cretaceous high-Mg# diorites from the Central Orogenic Block of the North China Craton: The nature of Mesozoic lithospheric mantle and constraints on lithospheric thinning. Chem Geol, 2010, 270: 257–273
26 Zhao G C, Sun M, Wilde S A, et al. Late Archean to Paleoproterozoic evolution of the North China Craton: Key issues revisited. Precambrian Res, 2005, 136: 177–202
27 Shandong Bureau of Geology and Mineral Resources (SBGMR). Regional Geology of Shandong Province (in Chinese). Ji'nan: Shandong Mapping Press, 2003. 331–350
28 Xu W L, Wang D Y, Wang Q H, et al. $^{40}Ar/^{39}Ar$ dating of hornblende and biotite in Mesozoic intrusive complex fromthe North China Block: Constraints on the time of lithospheric thinning (in Chinese). Geochemica, 2004, 33: 221–231
29 Yang C H, Xu W L, Yang D B, et al. Petrogenesis of Mesozoic high-Mg diorites in Western Shandong: Evidence from chronology and petro-geochemistry. J China Univ Geosci, 2005, 16: 297–308
30 Compston W, Williams I S, Kirschvink J L, et al. Zircon U-Pb ages for the Early Cambrian time-scale. J Geol Soc, 1992, 149: 171–184
31 Wi11iams I S. U-Th-Pb geochrono1ogy by ion microprobe, in Applications of Microanalytical Techniques to Understanding Mineralizing Processes. Rev Economic Geol, 1998, 7: 1–35
32 Song B, Zhang Y H, Wan Y S, et al. Mount making and procedure of the SHRIMP dating (in Chinese). Geol Rev, 2002, 48 (Suppl): 26–30
33 Black L P, Kamo S L, Allen C M, et al. TEMORA 1: A new zircon standard for Phanerozoic U-Pb geochronology. Chem Geol, 2003, 200: 155–170
34 Ludwig K R. User's Manual for Isoplot 3.00: A Geochronological Toolkit for Microsoft Excel. Berkeley: Berkeley Geochronological Center Special Publication, 2003. 4
35 Grieco G, Ferrario A, Quadt A V, et al. The zircon-bearing chromitites of the phlogopite peridotite of Finero (Ivrea zone, Southern Alps): Evidence and geochronology of a metasomatized mantle slab. J Petrol, 2001, 42: 89–101
36 Katayama I, Muko A, Lizuka S, et al. Dating of zircon from Ticlinohumite-bearing garnet peridotite: Implication for timing of mantle metasomatism. Geology, 2003, 31: 713–716
37 Zheng Y F, Yang J J, Gong B, et al. Partial equilibrium of radiogenic and stable isotope systems in garnet peridotite during ultra-high-pressure metamorphism. Am Mineral, 2003, 88: 1633–1643
38 Liati A, Franz L, Gebauer D, et al. The timing of mantle and crustal events in South Namibia, as defined by SHRIMP-dating of zircon domains from a garnet peridotite xenolith of the Gibeon Kimberlite Province. J Afr Earth Sci, 2004, 39: 147–157
39 Song S G, Zhang L F, Niu Y N, et al. Geochronology of diamond-bearing zircons from garnet peridotite in the North Qaidam UHPM belt, Northern Tibetan Plateau: A record of complex histories from oceanic lithosphere subduction to continental collision. Earth Planet Sci Lett, 2005, 234: 99–118
40 Zhang R Y, Yang J S, Wooden J L, et al. U-Pb SHRIMP geochronology of zircon in garnet peridotite from the Sulu UHP terrane, China: Implications for mantle metasomatism and subduction-zone UHP metamorphism. Earth Planet Sci Lett, 2005, 237: 729–743
41 Zheng J P, Griffin W L, O'Reilly S Y, et al. Zircons in mantle xenoliths record the Triassic Yangtze-North China continental collision. Earth Planet Sci Lett, 2006, 247: 130–142
42 Gao S, Rudnick R L, Yuan H L, et al. Recycling lower continental crust in the North China craton. Nature, 2004, 432: 892–897
43 Wu Y B, Zheng Y F. Genesis of zircon and its constraints on interpretation of U-Pb age. Chin Sci Bull, 2004, 49: 1554–1569
44 Koschek G. Origin and significance of the SEM cathodoluminescence from zircon. J Micros, 1993, 171: 223–232
45 Vavra G, Gebauer D, Schmid R, et al. Multiple zircon growth and recrystallization during polyphase Late Carboniferous to Triassic metamorphism in granulites of the Ivrea Zone (Southern Alps): An ion microprobe (SHRIMP) study. Contrib Mineral Petrol, 1996, 122: 337–358
46 Belousova E A, Griffin W L, O'Reilly S Y, et al. Igneous zircon: Trace element composition as an indicator of source rock type. Contrib Mineral Petrol, 2002, 143: 602–622
47 Hoskin P W O, Schaltegger U. The composition of zircon and igneous and metamorphic petrogenesis. Rev Mineral Geochem (Zircon), 2003, 53: 27–62
48 Xu Y G, Ma J L, Huang X L, et al. Early Cretaceous gabbrioc complex from Yinan, Shandong Province: Petrogenesis and mantle domains beneath the North China Craton. Int J Earth Sci (Geol Rundsch), 2004, 93: 1025–1041
49 Yang C H, Xu W L, Yang D B, et al. Chronology of the Jinan Gabbro in Western Shandong: Evidence from LA-ICP-MS Zircon U-Pb Dating (in Chinese). Acta Geosci Sin, 2005, 26: 321–325
50 Yang C H, Xu W L, Yang D B, et al. Petrogenesis of Shangyu gabbro-diorites in western Shandong: Geochronological and geochemical evidence. Sci China Ser D-Earth Sci, 2008, 51: 481–492
51 Xu W L, Wang Q H, Liu X C, et al. Chronology and sources of Mesozoic intrusive complex in Xu-Huai region, central China: Constraints from SHRIMP zircon U-Pb dating. Acta Geol Sin, 2004, 78: 96–106

52 Yang D B, Xu W L, Pei F P, et al. Chronology and Pb isotope compositions of Early Cretaceous adakitic rocks in Xuzhou-Huaibei area, central China: Constraints on magma sources and tectonic evolution in the eastern North China Craton (in Chinese). Acta Petrol Sin, 2008, 24: 1745–1758
53 Wang L G, Yiu Y M, McNaughton N J, et al. Constraints on crustal evolution and gold metallogeny in the Northwestern Jiaodong Peninsula, China, from SHRIMP U-Pb zircon studies of granitoids. Ore Geol Rev, 1998, 13: 275–291
54 Guo J H, Chen F K, Zhang X M, et al. Evolution of syn- to post-collisional magmatism from north Sulu UHP belt, eastern China: Zircon U-Pb geochronology (in Chinese). Acta Petrol Sin, 2005, 21: 1281–1301
55 Wu F Y, Lin J Q, Wilde S A, et al. Nature and significance of the Early Cretaceous giant igneous event in Eastern China. Earth Planet Sci Lett, 2005, 233: 103–119
56 Jiang Y H, Jiang S Y, Zhao K D, et al. SHRIMP U-Pb zircon dating for lamprophyre from Liaodong Peninsula: Constraints on the initial time of Mesozoic lithosphere thinning beneath eastern China. Chin Sci Bull, 2005, 50: 2612–2620
57 Yang D B, Xu W L, Wang Q H, et al. Chronology and geochemistry of Mesozoic granitoids in the Bengbu area, central China: Constraints on the tectonic evolution of the eastern North China Craton. Lithos, 2010, 114: 200–216
58 Wu F Y, Yang J H, Wilde S A, et al. Geochronology, petrogenesis and tectonic implications of the Jurassic granites in the Liaodong Peninsula, NE China. Chem Geol, 2005, 221: 127–156
59 Xu Y G, Chuang S L, Jahn B M, et al. Petrologic and geochemical constraints on the petrogenesis of Permian-Triassic Emeishan flood basalts in southwestern China. Lithos, 2001, 58: 145–168
60 He B, Xu Y G, Huang L X, et al. Age and duration of the Emeishan flood volcanism, SW China: Geochemistry and SHRIMP zircon U-Pb dating of silicic ignimbrites, post-volcanic Xuanwei Formation and clay tuff at the Chaotian section. Earth Planet Sci Lett, 2007, 255: 306–323
61 Wignall P B. Large igneous provinces and mass extinctions. Earth Sci Rev, 2001, 53: 1–33
62 Yang D B, Xu W L, Xu Y G, et al. Chronology of detrital zircons from Jurassic sandstones in western Shandong Province, China: Constraints on the nature of the Tan-Lu Fault Zone. Mineral Magazine, 2011, 75: 2207
63 Zhang S H, Zhao Y, Song B, et al. Carboniferous granitic plutons from the northern margin of the North China block: Implications for a late Paleozoic active continental margin. J Geol Soc Lond, 2007, 164: 451–463
64 Zhang S H, Zhao Y, Song B, et al. Contrasting Late Carboniferous and Late Permian-Middle Triassic intrusive suites from the northern margin of the North China craton: Geochronology, petrogenesis, and tectonic implications. Geol Soc Amer Bull, 2009, 121: 181– 200
65 Zhang S H, Zhao Y, Liu X C, et al. Late Paleozoic to Early Mesozoic mafic-ultramafic complexes from the northern North China Block: Constraints on the composition and evolution of the lithospheric mantle. Lithos, 2009, 110: 229–246
66 Zhao G C, Wilde S A, Li S Z, et al. U-Pb zircon age constraints on the Dongwanzi ultramafic-mafic body, North China, confirm it is not an Archean ophiolite. Earth Planet Sci Lett, 2007, 255: 85–93
67 Liu J M, Yang C H, Yang D B, et al. U-Pb chronology in zircon of magnetite-amphibolite intrusion from western Shandong and its geological implications (in Chinese). World Geol, 2006, 25: 221–228
68 Zhang H F, Ying J F, Tang Y J, et al. Phanerozoic reactivation of the Archean North China Craton through episodic magmatism: Evidence from zircon U-Pb geochronology and Hf isotopes from the Liaodong Peninsula. Gondwana Res, 2011, 19: 446–459
69 Dobbs P N, Duncan D J, Hu S, et al. The geology of the Mengyin kimberlites, Shandong, China. In: Meyer H O A, Leonardos O H, eds. Proceedings of the 5th International Kimberlite Conference 1. Diamonds: Characterization, Genesis and Exploration. Brasilia: CPRM, 1994. 106–115
70 Li Q L, Chen F K, Wang X L, et al. Single grain Rb-Sr isochronal dating of mica and its chemical processes with ultra-low background (in Chinese). Chin Sci Bull, 2006, 51: 321–325
71 Zhang H F, Yang Y H. Emplacement age and Sr-Nd-Hf isotopic characteristics of the diamondiferous kimberlites from the eastern North China Craton (in Chinese). Acta Petrol Sin, 2007, 23: 285–294
72 Tang Y J, Zhang H F, Nakamura E, et al. Multistage melt/fluid-peridotite interactions in the refertilized lithospheric mantle beneath the North China Craton: Constraints from the Li-Sr-Nd isotopic disequilibrium between minerals of peridotite xenoliths. Contrib Mineral Petrol, 2011, 161: 845–861
73 Liu Y S, Gao S, Hu Z C, et al. Continental and oceanic crust recycling-induced melt-peridotite interactions in the Trans-North China Orogen: U-Pb dating, Hf isotopes and trace elements in zircons from mantle xenoliths. J Petrol, 2010, 51: 537–571
74 Xu X S, Griffin W L, O'Reilly S Y, et al. Re-Os isotopes of sulfides in mantle xenoliths from eastern China: Progressive modification of lithospheric mantle. Lithos, 2008, 102: 43–64
75 Lu F X. Multiple-geological events of ancient lithospheric mantle beneath North China craton: As inferred from peridotite xenoliths in kimberlite (in Chinese). Acta Petrol Sin, 2010, 26: 3177–3188